

# The detection of dust grains by a wire dipole antenna: The Radio Dust Analyzer

Peter Meuris

Belgian Institute for Space Aeronomy, Brussels, Belgium

Nicole Meyer-Vernet

Département Recherches Spatiales, Observatoire de Paris, Meudon, France

Joseph F. Lemaire

Belgian Institute for Space Aeronomy, Brussels, Belgium

**Abstract.** The possibility of a wire dipole antenna to study the characteristics of dust grains is examined. Charged dust grains passing by the antenna induce an electric potential change for the time of the flyby. These “waveforms” are studied as a function of the characteristics of the dust grain (its charge and velocity vector) and the plasma parameters. The thermal noise level due to flyby, emission, and impacts of the ambient plasma electrons is calculated and compared with the magnitude of the dust signal. Qualitative analysis yields a minimum detectable grain size, the minimum antenna sensitivity required, and the number of detectable events per time unit for cometary, planetary, and interplanetary environments. We call this recently proposed dust-detection technique Radio Dust Analyzer (RDA).

## 1. Introduction

A dusty plasma consists of dust particles coupled to the ambient plasma through existing or self-induced electromagnetic fields. Depending upon the concentration, one has isolated screened dust grains (dust-in-plasma) or real dusty plasmas, when the charged dust participates in the Debye screening. Comprehensive reviews have been given by Goertz [1989], Northrop [1992], Mendis and Rosenberg [1994], and Verheest [1996]. The study of dusty plasmas is a relatively new area of research with respect to theoretical development as well as specific applications. Recent interest in such plasmas has increased because of observation of dust in the vicinity of comets and in laboratory devices. But much of the characteristics of the dust in space are still unknown.

Remote-sensing methods like light scattering by the dust at different angles, absorption of radiowaves, and stellar occultation measurements have led to most of our knowledge of planetary rings. In recent missions (Galileo and Ulysses), direct measurements were made by a dust detector [Grün *et al.*, 1992a b], while in this paper we examine the use of a wire dipole antenna to examine some dust characteristics from the antenna response on a grain flyby. Although antennas were used before in the detection of dust grains by impact ionization [Gurnett *et al.*, 1987; Meyer-Vernet *et al.*,

1986], this method requires sufficient kinetic energy to ionize the grain and thus works only for grain-antenna velocities larger than several kilometers per second. On the other hand, the Radio Dust Analyzer (RDA) works best for small velocities because the signal is not hidden by impact ionization, and the waveform does not require a good time resolution to be detected. This paper, which is based on previous work for a sphere dipole antenna [Lesceux *et al.*, 1987], is organized as follows. In section 2 the basic theoretical framework is given and the grain’s “signature” is examined. Sections 3 contains a discussion of the noise level due to plasma particles flying by the antenna, while section 4 discusses the noise level due to direct emission and collection by the antenna. The practical use of RDA is discussed in section 5 for three different types of environments corresponding to existing or future space missions. Section 6 gives our conclusions.

## 2. Theory

We consider a maxwellian two-component plasma, with electron and ion temperature  $T_e = T_i = T$  and plasma density  $N$ . The electron Debye length is given by

$$\lambda_D^2 = \frac{\epsilon_0 \kappa T}{Ne^2}, \quad (1)$$

where  $\epsilon_0$  is the vacuum permittivity and  $\kappa$  is Boltzmann’s constant. A spherical dust grain with radius  $a \ll \lambda_D$  and scalar velocity  $v$  embedded in the plasma acquires an equilibrium charge  $Q$ , given by the standard charging model

Copyright 1996 by the American Geophysical Union.

Paper number 96JA02490.  
0148-0227/96/96JA-02490\$09.00

[Northrop, 1992]. The constant charge assumption is valid in the regime where the charge variation timescale is larger than the dust signature width. In all cases of practical interest, the velocity satisfies  $v \ll v_{se}$  ( $v_{s\alpha}$  denotes the thermal velocity of species  $\alpha$ ), so that the electrons contribute fully to the shielding. When  $v_{si} \ll v \ll v_{se}$ , the ions do not contribute at all and the relevant Debye length is  $\lambda_D$  (this would remain true when  $v$  is of order of magnitude  $v_{si}$  provided that  $T_e \ll T_i$ ). If on the other hand  $v \ll v_{si} \ll v_{se}$ , the ions and electrons fully shield the charge and the relevant Debye length becomes  $\lambda_D/\sqrt{2}$ . In intermediate cases, the plasma temporal dispersion cannot be neglected and the problem is more complicated. The well-known Debye-shielded potential around one single dust grain is then given by

$$\Phi(r) = \Phi_0 \frac{a}{r} e^{-(r-a)/\lambda_D}, \quad (2)$$

$$\Phi_0 = \Phi(a) = \frac{Q}{4\pi\epsilon_0 a}, \quad (3)$$

keeping in mind that when  $v \ll v_{si}$ ,  $\lambda_D$  must be replaced by  $\lambda_D/\sqrt{2}$  and that we have implicitly assumed linear shielding, i.e.,  $\Phi(r) \ll \kappa T/e$ , which is always satisfied in practice.

We consider a Cartesian  $(x, y, z)$  frame and a wire dipole antenna (with radius  $r_a$ ) positioned along the  $z$  axis, with the two arms (each arm with length  $L$ ) meeting each other in the origin (Figure 1). Furthermore we assume that the response time of the receiver antenna system is much smaller than the dust flyby time, and that the antenna is thin enough ( $r_a \ll L$  and  $r_a \ll \lambda_D$ ). The dust signature width has a value intermediate between the time for a grain moving parallel to the antenna  $(L + \lambda_D)/v$  and that for a grain moving perpendicular to the antenna  $(\lambda_D/v)$ .

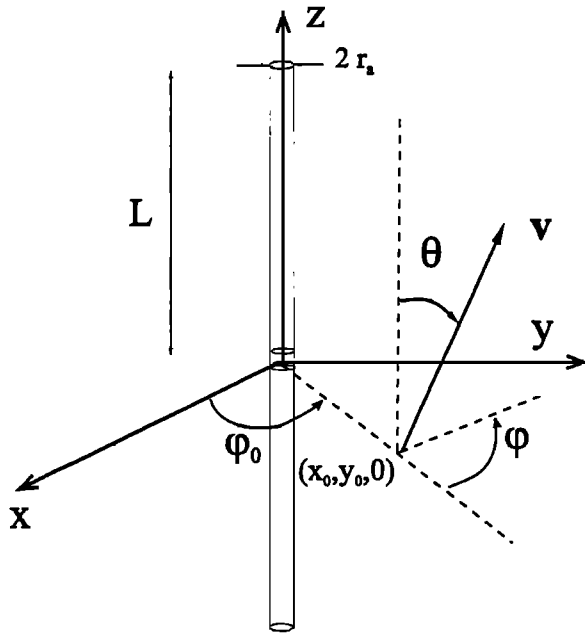


**Figure 1.** Antenna geometry of a wire dipole antenna and the coordinates used.

The orbit of a dust grain in uniform motion is given by

$$x(t) = x_0 + v \sin(\theta) \cos(\varphi + \varphi_0) t \quad (4)$$

$$y(t) = y_0 + v \sin(\theta) \sin(\varphi + \varphi_0) t \quad (5)$$

$$z(t) = z_0 + v \cos(\theta) t, \quad (6)$$

where  $(v, \theta, \varphi)$  are the spherical coordinates of the velocity of the grain relative to the antenna as indicated in Figure 1.

The potential at a point  $(x, y, z)$  on the antenna is given by

$$\Phi[x, y, z, t] = \frac{a}{R} \Phi_0 e^{-\frac{R}{\lambda_D}}, \quad (7)$$

with

$$R = \sqrt{[x(t) - x]^2 + [y(t) - y]^2 + [z(t) - z]^2}. \quad (8)$$

The voltage measured by a wire dipole antenna is the difference between the voltages averaged over each arm; hence the antenna response is

$$\Delta\Phi(t) = \frac{1}{L} \int_{-L}^0 \Phi[0, 0, z, t] dz - \frac{1}{L} \int_0^L \Phi[0, 0, z, t] dz. \quad (9)$$

According to (9), the antenna response  $\Delta\Phi(t)$  is proportional to  $\Phi_0 a$  and hence to  $Q$ . We introduce the shape function

$$\xi(t) = \frac{\Delta\Phi(t)}{a\Phi_0}, \quad (10)$$

with dimensions in  $m^{-1}$ . The problem depends on the six geometrical parameters  $v, \theta, \varphi, \varphi_0, r_0 = \sqrt{x_0^2 + y_0^2}, z_0$  of the grain's orbit. Changing  $\varphi_0$  will not change the antenna response due to the cylindrical symmetry. Since  $v$  is only present in the expression  $vt$ , changing  $v$  will only stretch the timescale and will not change the shape of the shape function. When we take  $t = 0$  when  $z = 0$ , there are just three parameters left to determine the shape:  $\theta, \varphi$ , and  $r_0$ .

Given a response profile, it is theoretically possible to fit the parameters  $v, \theta, \varphi, r_0$ , and  $\Phi_0 a \propto Q$ . Furthermore, in most of the cases we already know the direction of the dust-antenna velocity and even its magnitude. In that case the problem becomes a fit for  $r_0, \varphi$ , and  $\Phi_0 a \propto Q$ . A complete description of a method to compute such parameters from the waveform will be given in a future paper. Here we are only giving some indications of the relations between the features of the waveform and the values of those parameters. The results might be generalized to a more complex antenna system (triple or quadrupole), in order to refine the diagnostics.

Figure 2 shows the normalized potential distribution on the  $z$  axis for a grain in the  $x - y$  plane. In this particular case, the resulting antenna response is zero, because  $\Phi$  is symmetrical in  $z$ . When the grain moves parallel to the antenna, the shape of the curve does not change, but the maximum is found at the current  $z$  value of the grain. Hence a nonvanishing signal is produced.

In Figure 3a the shape function for a grain moving parallel to the antenna is shown for different antenna lengths.

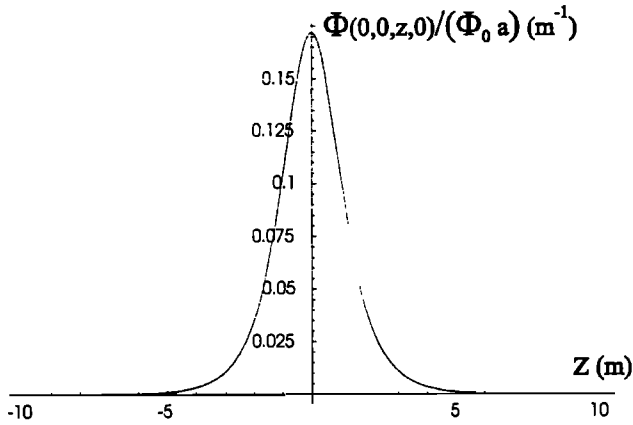


Figure 2. Normalized potential along the  $z$  axis for a grain in the  $x - y$  plane at a distance of  $r_0 = 1.41$  m from the antenna.  $L = 10$  m,  $\lambda_D = 1$  m.

Increasing the antenna length increases the width of the signal, as expected, while the response reaches a maximum for a specific antenna length.

Figure 3b shows the influence of the Debye length for a grain moving parallel to the antenna. It is readily understood that the regime where  $\lambda_D \ll L$  gives no response at all, because of Debye shielding of the grain charge. However, when we increase the Debye length, the maximum response increases and eventually reaches a constant value.

Figure 3c shows the influence of the orbit's orientation with  $\theta$  in the first quadrant. For  $\theta$  in the other quadrants, these results can be used by taking into account the transformations  $\theta \rightarrow \theta + \pi \Leftrightarrow t \rightarrow -t$  and  $\theta \rightarrow \pi - \theta \Leftrightarrow \xi(t) \rightarrow -\xi(t)$ . The influence of  $\varphi$  is shown in Figure 3d with values taken in the first quadrant.

Figure 3e shows the influence of  $r_0$ . When  $r_0 \gg \lambda_D$ , the antenna response becomes very small.

The practical use of antennae as grain detectors has several limitations: first of all, the random voltage induced by the plasma particles passing near the antenna, examined in section 3, and second the random voltage induced on the antenna by particle impacts and/or emissions, examined in

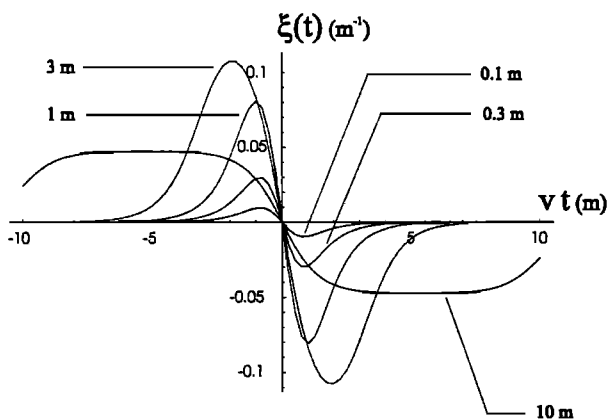


Figure 3a. Antenna response for a grain moving parallel to the antenna as a function of  $vt$  for different antenna lengths. Here  $r_0 = 1.41$  m,  $\lambda_D = 1$  m.

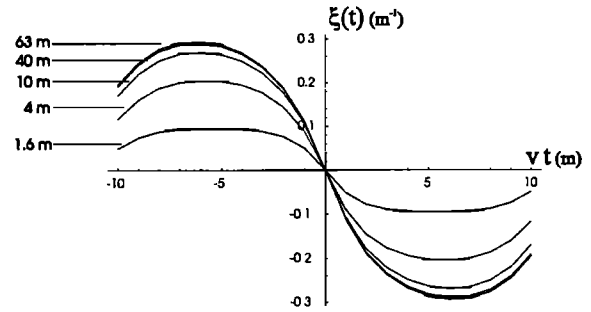


Figure 3b. Antenna response for a grain moving parallel to the antenna as a function of  $vt$  for different Debye lengths. Here  $r_0 = 1.41$  m,  $L = 10$  m.

section 4. Both noises have to be smaller than the dust signal for it to be detectable. The magnitude of the signature of the grain itself is proportional to its size and equilibrium potential of the grain (of the order of the thermal energy of the main charging process [Northrop, 1992]) and to the shape function.

### 3. Noise Level Due to Plasma Particle Flyby

Together with the grain signature on the antenna we would expect a contribution ( $\Phi_P(t)$ ) due to the flyby of the plasma particles. Owing to the nonzero time constant of the receiver, the antenna does not "see" individual electrons but a mean over a large number of passages. The signal produced by a single flyby for a plasma particle of velocity  $v$  is an odd function of  $v$ . The average of such a signal over a Maxwellian distribution yields  $\langle \Phi_P(t) \rangle = 0$ .

So we calculate the variance  $\langle \Phi_P^2(t) \rangle$ , given for Maxwellian electrons and ions, by [Meyer-Vernet and Perche, 1989]

$$\langle \Phi_P^2(t) \rangle = \int_0^\infty \langle \Phi_P^2(f) \rangle df, \quad (11)$$

where  $\Phi_P^2(f)$  is the noise spectral density:

$$\langle \Phi_P^2(f) \rangle = 4\kappa T \operatorname{Re}(Z), \quad (12)$$

$$Z = \frac{4i}{\pi^2 \epsilon_0 \omega} \int_0^\infty \frac{F(k)}{\epsilon_L(k, \omega)} dk, \quad (13)$$

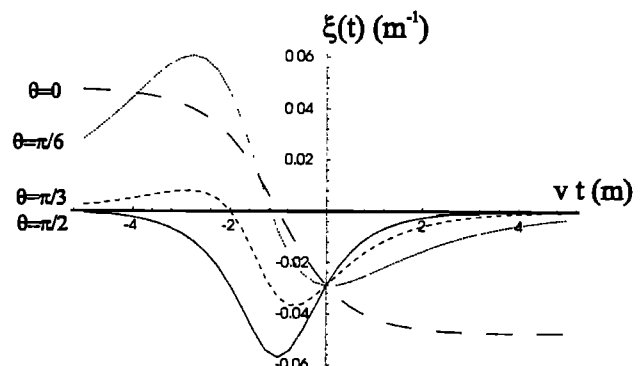


Figure 3c. Antenna response as a function of  $vt$  for different  $\theta$ . Here  $r_0 = 1.41$  m,  $\varphi = -\pi/4$ ,  $L = 10$  m,  $\lambda_D = 1$  m.

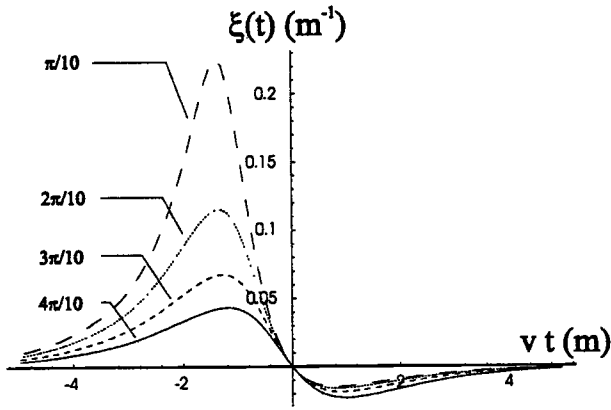


Figure 3d. Antenna response as a function of  $vt$  for different  $\varphi$ . Here  $r_0 = 1$  m,  $\theta = \pi/2$ ,  $L = 10$  m,  $\lambda_D = 1$  m.

$$F(k) = \frac{1}{32\pi} \int |\mathbf{k} \cdot \mathbf{J}(\mathbf{k})|^2 d\Omega \quad (14)$$

$$= \left( \frac{\text{Si}(kL)}{kL} - \frac{\text{Si}(2kL)}{2kL} - \frac{2 \sin^4(kL/2)}{k^2 L^2} \right). \quad (15)$$

Here  $\epsilon_L$  is the longitudinal permittivity,  $\epsilon_0$  is the vacuum permittivity and  $Z$  is the antenna impedance. Si denotes the sine integral function. In (14) the integration is over the direction of  $\mathbf{k}$ .

To evaluate these integrals, we assumed a linear current distribution:

$$\mathbf{J}(\mathbf{k}) = \frac{4}{k_z^2 L} \sin^2(k_z L/2) [J_0(k_r r_a)] \mathbf{e}_z, \quad (16)$$

with  $k^2 = k_z^2 + k_r^2$ . The noise variance is then given (for  $r_a \ll L$  and  $r_a \ll \lambda_D$ ):

$$\langle \Phi_P^2(t) \rangle = \frac{4\kappa T}{\pi^2 \epsilon_0} \int_0^\infty \frac{F(k)}{1 + k^2 \lambda_D^2/2} dk. \quad (17)$$

Unlike the case of a spherical dipole antenna, evaluating this integral analytically is not easy. We restrict this paper to a numerical evaluation of (17). With the help of the change of variables  $y = k\lambda_D/\sqrt{2}$ , the noise variance due to plasma particle flyby can be put in the form

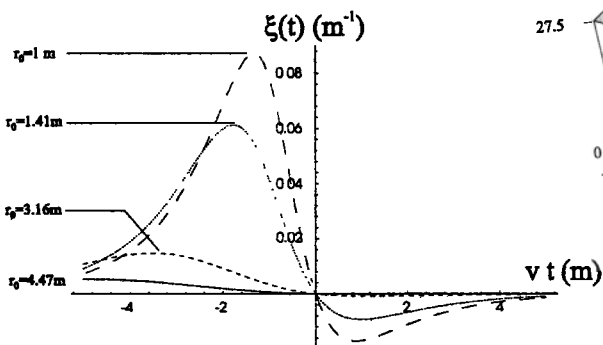


Figure 3e. Antenna response as a function of  $vt$  for different  $r_0$ . Here  $\varphi = -\pi/4$ ,  $\theta = \pi/4$ ,  $L = 10$  m,  $\lambda_D = 1$  m.

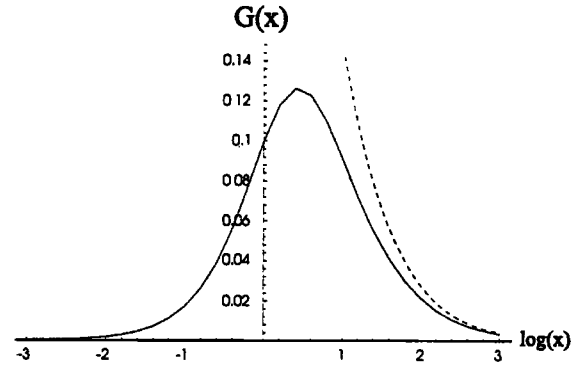


Figure 4. Plot of the function  $G(x)$  in full line. The dashed line indicates the analytical result for  $x \gg 1$ .

$$\langle \Phi_P^2(t) \rangle = \frac{4\sqrt{2}\kappa T}{\pi^2 \epsilon_0 \lambda_D} G(L/\lambda_D). \quad (18)$$

Increasing the Debye length decreases the noise. Indeed, when the Debye length increases, three phenomena occur. The timescale for a single plasma particle flyby and the number of relevant plasma particles both increase because of the bigger Debye sphere around the particle. However, the amplitude of the mean plasma particle signal decreases. This is due to the decrease of the average magnitude of the responses, which is proportional to the inverse of the mean distance of the flyby's, given by the Debye length.

The effect of the antenna length is illustrated in Figure 4, which shows the function  $G(x)$  in full line. The response of a wire dipole antenna reaches a maximum for wave vectors satisfying  $k_z \approx 3/L$ . This results in a variance that reaches a maximum for a specific antenna length  $L_M$ , given by the maximum of the function  $G(x)$  located at  $L_M = 2.74 \lambda_D$ . The analytical result for the case  $\lambda_D \ll L$ ,

$$\langle \Phi_P^2(t) \rangle = \frac{\kappa T}{\pi \epsilon_0 L} \ln(\sqrt{2}L/\lambda_D), \quad (19)$$

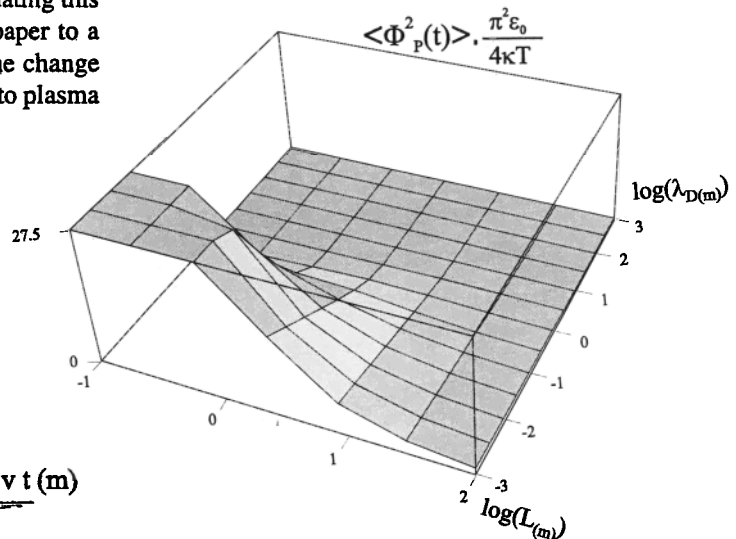


Figure 5. Normalized noise variance due to plasma particles flyby, as a function of the antenna length and Debye length,  $T$  being constant.

is shown in Figure 4 as a dashed line. Figure 5 shows the normalized noise as a function of  $L$  and  $\lambda_D$ .

#### 4. Noise Level Due to Plasma Particle Impacts or Emissions

If the antenna is not meshed, it can collect or emit particles, which gives rise to a noise ( $\Phi_{i/e}(t)$ ). In general, the problem is very complicated [Calder and Laframboise, 1985]. The number of impacts or emissions cannot be determined exactly, because it depends on the unknown floating potential and surface state of the antenna. However, an order of magnitude of the resulting noise variance can be calculated as follows.

One event, i.e., one electron impact (or emission), on one antenna arm produces the voltage maximum amplitude given by  $[e/(2C)]^2$ , where  $C$  stands for the capacitance of the antenna given by

$$C = \frac{\pi\epsilon_0 L}{\ln(\lambda_D/r_a)}. \quad (20)$$

This voltage squared has to be multiplied by the number of events per time unit and by a typical timescale in order to obtain the variance. The number of events per time unit is given by  $2I_e/e$ , where  $I_e$  stands for the electron current to the antenna. The factor 2 takes into account the return current.

Indeed, the equilibrium potential is a result of the balance ( $|I_p|+|I_i|=|I_e|$ ) between electron and ion currents and photoelectron current  $I_e$ ,  $I_i$  and  $I_p$ , so that the number of events ( $|I_e|+|I_i|+|I_p|)/e$  can be simplified to  $2|I_e|/e$ .

A typical timescale is the decay time of the signal given by  $\tau = RC$ . Since the antenna is not meshed, the resistance  $R$  is mainly due to the dc current. In order of magnitude, this dc resistance  $R_{dc}$  is given by the inverse of the derivative of the dc current on the antenna:

$$\frac{1}{R_{dc}} \approx \left| \frac{dI}{d\Phi} \right| \approx \frac{I_e e}{\kappa T_{ef}}. \quad (21)$$

For a negative antenna potential, only the direct plasma current contributes to  $R_{dc}$  and  $T_{ef} = T$ , while for a positive antenna potential, the photoelectron current contributes and the order of magnitude of the effective temperature is then given by  $1/T_{ef} = 1/T + 1/T_p$ , where  $T_p$  is the temperature of the photoelectrons ( $\sim 1$  eV) [Goertz, 1989].

Hence the order of magnitude of the noise variance is given by

$$\langle \Phi_{i/e}^2(t) \rangle \approx \left( \frac{e}{2C} \right)^2 \frac{2I_e}{e} C \frac{\kappa T_{ef}}{eI_e} \quad (22)$$

$$= \frac{\kappa T_{ef}}{2C} \quad (23)$$

$$= \frac{\kappa T_{ef} \ln(\lambda_D/r_a)}{2\pi\epsilon_0 L}. \quad (24)$$

Figure 6 shows this noise level as a function of  $L$  and  $\lambda_D$ .

#### 5. The Practical Use of RDA

To be able to detect grains with RDA, the grain signal has to be larger than the noise levels. Also, for the response to be detectable, the signal should be larger than the sensitivity of the receiver. The first condition gives a minimum detectable grain size:

$$a_m = \frac{\text{Max} \left[ \sqrt{\langle \Phi_{i/e}^2(t) \rangle}, \sqrt{\langle \Phi_P^2(t) \rangle} \right]}{(\xi_M \Phi_0)}, \quad (25)$$

$\xi_M$  being the maximum value of the shape function for a typical grain flyby at a distance  $r_0 = \lambda_D$ , for  $\theta = \varphi = \pi/4$ . The second condition gives the sensitivity needed to detect the smallest detectable grains:

$$\Delta \Phi_s = a_m \Phi_0 \xi_M \quad (26)$$

$$= \text{Max} \left[ \sqrt{\langle \Phi_{i/e}^2(t) \rangle}, \sqrt{\langle \Phi_P^2(t) \rangle} \right]. \quad (27)$$

The number of detectable events per time unit is given by  $f = vN_d S$ , where  $N_d$  denotes the number density of detectable grains and  $S$  is the cross section of the detector. The latter is given by

$$S = 4\lambda_D [\lambda_D \pi \cos(\theta) + L \sin(\theta)]. \quad (28)$$

Results are shown in Table 1 for a selection of cases in cometary, interplanetary, and planetary media, which might be useful in the Rosetta, Wind, and Cassini missions respectively.

##### 5.1. Cometary Medium

To get estimates for a cometary medium, we use results for comet P/Hartley 2 near perihelion ( $\sim 1$  AU) from *McDonnell et al.* [1992] and extrapolate them for comet P/Wirtanen, which will be visited by the Rosetta mission. We

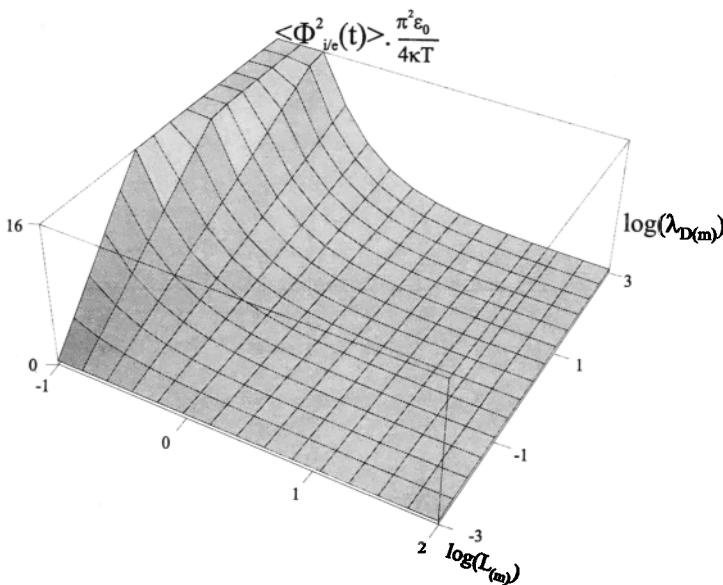


Figure 6. Normalized noise variance due to plasma particles impacts and/or emission, as a function of the antenna length and Debye length, for a fixed  $r_a = 1$ mm,  $T$  being constant.

**Table 1.** The Equivalent Cross Section of the Detector ( $S$ ), the Noise Levels, the Minimum Detectable Grain Radius ( $a_m$ ), the Minimum Antenna Sensitivity Required to Detect the Smallest Detectable Grains ( $\Delta\Phi_s$ ) and the Event Rate ( $f$ ) Given for Different Types of Environments, With Typical Plasma ( $\lambda_D, T$ ), Grain ( $\Phi_0, N_d, v$ ) and Antenna ( $L, r_a$ ) Parameters

	Case 1	Case 2	Case 3	Case 4
$\lambda_D, \text{m}$	10	0.1	7.5	10
$T, \text{K}$	$100 \times 10^3$	100	$100 \times 10^3$	$100 \times 10^3$
$\Phi_0, \text{V}$	10	10	7.5	-20
$N_d, \text{m}^{-3}$	$10^{-5} \text{ }^a$	$3 \times 10^{-2} \text{ }^a$	$1.5 \times 10^{-14} \text{ }^b$	—
$v, \text{m s}^{-1}$	100	100	$20 \times 10^3$	$10 \times 10^3$
$L, \text{m}$	5	5	40	10
$r_a, \text{m}$	$1.0 \times 10^{-3}$	$1.0 \times 10^{-3}$	$2.0 \times 10^{-3}$	$14 \times 10^{-3}$
$S, \text{m}^2$	$1.1 \times 10^3$	2.0	$1.4 \times 10^3$	$1.2 \times 10^3$
$\xi_M, \text{m}^{-1}$	0.03	0.2	0.04	0.1
$\sqrt{\langle \Phi_{i/e}^2(t) \rangle}, \text{V}$	$7 \times 10^{-5}$	$5 \times 10^{-6}$	$2 \times 10^{-5}$	$4 \times 10^{-5}$
$\sqrt{\langle \Phi_p^2(t) \rangle}, \text{V}$	$2 \times 10^{-5}$	$6 \times 10^{-6}$	$4 \times 10^{-5}$	$3 \times 10^{-5}$
$a_m, (\mu\text{m})$	250	3	150	20
$\Delta\Phi_s, \mu\text{V}$	70	6	40	40
$f, \text{s}^{-1}$	1	6	$4 \times 10^{-7}$	$12 \times 10^6 N_d$

The value of  $\xi_{maz}$  is given for a grain flyby at a distance  $r_0 = \lambda_D$ , for  $\theta = \varphi = \pi/4$ . Case 1, Cometary environment, outside the contact surface. Case 2, Cometary environment, inside the contact surface. Case 3, Interplanetary medium at 1 AU heliospheric distance. Case 4, Planetary environment, Saturn's dilute E-ring.

<sup>a</sup>Cumulative density for grains larger than  $a_m$ ; adapted from *McDonnell et al.* [1992]

<sup>b</sup>[*Grün et al.*, 1985]

take a gas production rate typically 3 times lower, assume the same dust to gas ratio, and consider a distance from the nucleus of 100 km. The flux of particles of mass  $m \approx 10^{-10} - 10^{-9}$  kg (corresponding to  $a_m$  of case 2 in Table 1) is then  $F = 3 \text{ m}^{-2} \text{ s}^{-1}$ . This corresponds to a dust density of  $N_d \sim 0.03 \text{ m}^{-3}$ . The corresponding event rate is of the order of one event per second.

To get an estimate for particles of mass  $m > 10^{-6}$  kg (corresponding to  $a_m$  of case 1), we assume a grain mass distribution such that the flux of particles with mass  $m > m_0$ , is proportional to  $m_0^{-4/5}$ . This exponent is close to the mean value measured in situ for comet P/Halley [*McDonnell et al.*, 1987], and to recent measurements for large grains in two other comets [*Fulle*, 1992; *Fulle et al.*, 1992]. The flux is then  $F \sim 10^{-3} \text{ m}^{-2} \text{ s}^{-1}$  and the corresponding dust density is  $N_d \sim 10^{-5} \text{ m}^{-3}$ . Again, the corresponding event rate is of the order of one event per second. Note that if the grains are fluffy, the charge mass ratio is larger, which would significantly decrease the minimum size of detectable grains and thus increase the event rate.

## 5.2. Interplanetary Medium

Table 1 of *Grün et al.* [1985] gives the cumulative lunar flux for different models. This flux is close to the average interplanetary flux at 1 AU, for the considered particle sizes.

With the value of  $a_m$  given in case 3, the minimum mass of detectable particles is of the order of  $10^{-7}$  kg, for a grain density of  $2.5 \times 10^3 \text{ kg m}^{-3}$ . This corresponds to an event rate of  $f = 4 \times 10^{-7} \text{ s}^{-1}$  and a typical time between the events of about a month.

However, if the grain mass density, like often suggested for large grains, is smaller than  $2.5 \times 10^3 \text{ kg m}^{-3}$ ,  $f$  would increase. The same happens within sporadic meteoroid streams.

## 5.3. Planetary Medium

In planetary media, we should use RDA outside the ring plane, in order to ensure that the signal is not hidden by impact ionization. Hence to evaluate the event rate, we need dust data outside the known rings. Because these data are barely available, we restrict our analysis to  $a_m$  and  $\Delta\Phi_s$ .

## 6. Conclusions

A new method (RDA) is given to detect the electric charge and most elements of the velocity vector of dust grains in space plasmas. This method is complementary to detection by impact ionization: the latter requires sufficient kinetic energy to ionize the grain and thus works only for grain-spacecraft velocities larger than several  $\text{km s}^{-1}$ , whereas

the RDA works best for small velocities. The advantage of this detector with respect to impact ionization or to conventional dust detectors is its large cross section: of the order of  $4\lambda_D \text{Max}(\lambda_D, L)$ , instead of the physical surface of the detector. On the other hand, the signal is in general very weak, so that the method requires a sensitive receiver.

Strong indications are given for the possible use of this technique. Case studies indicate that grains of size exceeding  $a_m$  can be detected with a receiver with sensitivity larger than  $\Delta\Phi_s$ . The event rate is also calculated, giving values of the order of one event per second for cometary environments and one event per month for a typical interplanetary environment.

A complete description of a method to compute the dust characteristics from the antenna response is not given here but will be worked out in a future paper. The diagnostics can become more accurate, using a more complex antenna system (triple or quadrupole). But this is by no means trivial because of the corresponding decrease in the cross section of the analyzer for coincidence measurements.

**Acknowledgments.** For PM this text presents research results of a program initiated by the Belgian State, Prime Minister's Office, and the Federal Office for Scientific, Technical and Cultural Affairs. P.M. and J.L. thank the director of the BISA, Baron Ackerman, for giving them the opportunity to work at the Belgian Institute for Space Aeronomy. We are grateful to D. Bockelee-Morvan, J. L. Bougeret, D. Gurnett, M. Roth, and F. Verheest for many interesting discussions.

The editor thanks Eberhard Grün and Donald A. Gurnett for their assistance in evaluating this paper.

## References

- Calder, A. C., and J. G. Laframboise, Terminal properties of a spherical RF electrode in an isotropic Vlasov plasma: Results of a computer simulation, *Radio Sci.*, 20, 989–999, 1985.
- Fulle, M., Dust from short period comet P/Schwassmann-Wachmann 1 and replenishment of the interplanetary dust cloud, *Nature*, 359, 42–44, 1992.
- Fulle, M., G. Cremonese, K. Jockers, and H. Rauer, The dust tail of comet Liller 1988 V, *Astron. Astrophys.*, 253, 615–624, 1992.
- Goertz, C.K., Dusty plasmas in the solar system, *Rev. Geophys.*, 27, 271–292, 1989.
- Grün, E., H.A. Zook, H. Fechtig, R.H. Giese, Collisional balance of the meteoritic complex, *Icarus*, 62, 244–272, 1985.
- Grün, E., H. Fechtig, R.H. Giese, J. Kissel, D. Linkert, D. Maas, J.A.M. McDonnell, G.E. Morfill, G. Schwem, and H.A. Zook, The Galileo dust detector, *Astron. Astrophys. Suppl. Ser.*, 92, 411–423, 1992a.
- Grün, E., H. Fechtig, M.S. Hanner, J. Kissel, B.-A. Lindblad, D. Linkert, G. Linkert, G.E. Morfill and H.A. Zook, The Galileo dust detector, *Space Sci. Rev.*, 60, 317–340, 1992b.
- Gurnett, D.A., W.S. Kurth, W.S. Scarf, J.A. Burns, J.N. Cuzzi and E. Grün, Micron-sized particle impacts detected near Uranus by the Voyager 2 plasma wave instrument, *J. Geophys. Res.*, 92, 14959–14968, 1987.
- Lesceux, J.M., J. Lemaire and N. Meyer-Vernet, Electric dipole antennae used as micrometeoroid detectors, *Planet. Space Sci.*, 37, 1291–1301, 1987.
- McDonnell, J.A.M. et al., The dust distribution within the inner coma of comet P/Halley 1982i: - Encounter by Giotto's impact detector, *Astron. Astrophys.*, 187, 719–741, 1987.
- McDonnell, J.A.M., R. Beard, S.F. Green, and G.H. Schwehm, Cometary coma particulate modelling for the ROSETTA mission aphelion rendezvous, *Ann. Geophys.*, 10, 150–156, 1992.
- Mendis, D.A. and M. Rosenberg, Cosmic dusty plasma, *Annu. Rev. Astron. Astrophys.*, 32, 419–463, 1994.
- Meyer-Vernet, N. and C. Perche, Tool kit for antennae and thermal noise near the plasma frequency, *J. Geophys. Res.*, 94, 2405–2415, 1989.
- Meyer-Vernet, N., M.G. Aubier, and B.M. Pedersen, Voyager-2 at Uranus: Grain impacts in the ring plane, *Geophys. Res. Lett.*, 13, 617–620, 1986.
- Northrop, T.G., Dusty plasmas, *Phys. Scr.*, 45, 475–490, 1992.
- Verheest, F., Waves and instabilities in dusty space plasmas, *Space Sci. Rev.*, in press, 1996.

---

Joseph F. Lemaire and Peter Meuris, Belgian Institute for Space Aeronomy, Ringlaan 3, B-1180 Brussels, Belgium. (e-mail: jl@oma.be; peter.meuris@oma.be)

Nicole Meyer-Vernet, Département Recherches Spatiales, Observatoire de Paris, 92195 Meudon, France. (e-mail: meyer@megasv.obsprm.fr)

(Received February 1, 1996; revised June 24, 1996; accepted August 9, 1996.)